Applied Catalysis B: Environmental 142–143 (2013) 112–118

Contents lists available at SciVerse ScienceDirect

Applied Catalysis B: Environmental

journal homepage: www.elsevier.com/locate/apcatb

Effect of the nature of the support on the activity of Pt-Sn based catalysts for hydrogen production by dehydrogenation of Ultra Low Sulfur Kerosene Jet A-1

Mélanie Taillades-Jacquin[a,*], Carlo Resini[a], Kan-Ern Liew[a,b], Gilles Taillades[a], Ilenia Gabellini[c], David Wails[c], Jacques Rozière[a], Deborah Jones[a]

[a] Institut Charles Gerhardt UMR 5253, Agrégats, Interfaces et Matériaux pour l'Energie, Université Montpellier 2, Place Eugène Bataillon, 34095 Montpellier cedex 5, France
[b] Power Generation, EADS Innovation Works, Dept. IW-EP, Energy & Propulsion, 81663 Munich, Germany
[c] Johnson Matthey Technology Centre, Blount's Court, Sonning Common, Reading, RG4 9NH, United Kingdom

ARTICLE INFO

Article history:
Received 5 October 2012
Received in revised form 13 February 2013
Accepted 18 February 2013
Available online 26 February 2013

Keywords:
Hydrogen production
Partial dehydrogenation
Ultra Low Sulfur Kerosene
Pt-Sn/Al_2O_3 based catalysts
Catalyst support influence

ABSTRACT

Production of hydrogen on-board an airplane, to feed a fuel cell secondary power generation unit, is realisable by catalytic partial dehydrogenation of kerosene. The influence of the nature support on the partial dehydrogenation of Ultra Low Sulfur Kerosene Jet A-1 using Pt-Sn based catalysts is investigated in this work. The doping of an alumina support with barium oxide leads to a catalyst providing a productivity of 2000 NL_{H2} kg_{cat}^{-1} h^{-1} with H_2 purity of 97 vol.%.

1. Introduction

There is a global motivation to develop greener technologies in transport applications and new developments in the electrification of aircraft technology represent an opportunity to reduce greenhouse gas (GHG) emissions. Among new methodologies, efficient on-board generation of hydrogen to feed a fuel cell secondary power generation unit would avoid problems of hydrogen storage and transport. On-board H_2 production attracts increasing interest [1–5] and the most promising method is the dehydrogenation of chemical hydrides, high hydrogen containing cyclic hydrocarbons, as their hydrogen storage capacity may lie in the range 6–8 wt% [4], and as their hydrogenation and dehydrogenation are reversible [4,6–9]. On-board the aircraft, the use of kerosene as source of hydrogen is of great interest [10] as the lack of oxygen in the kerosene composition makes it suitable for partial dehydrogenation to produce dehydrogenated hydrocarbons in the liquid phase and hydrogen in the gas phase. The hydrogen is free of CO and CO_2 and so can directly feed an on-board proton exchange membrane fuel cell (PEMFC) for supply of electrical energy to auxiliary systems, without a purification step. The liquid phase, composed of partially dehydrogenated hydrocarbons, maintains its original fuel properties with the requisite specifications to be used as jet fuel. Noble metal and bimetallic catalysts, particularly with platinum and another metal have been investigated and reported to be active in the dehydrogenation of cycloalkanes [4,6,7,11,12]. Various supports for Pt-containing catalysts have been investigated [4,7,11–13] and the different studies show the key role played by the support.

The choice of the catalyst is crucial for the partial dehydrogenation process; it must produce H_2 without compromising the original fuel properties. An ideal catalyst must be sulfur tolerant, generate sufficient hydrogen of high purity, be selective to dehydrogenation and avoid cracking reactions responsible for coke deposition and catalyst deactivation. Bimetallic Pt–Sn/γ-Al_2O_3 based catalysts have been studied and reported in the literature. The presence of tin restricts sintering of Pt clusters, improves catalyst stability towards deactivation by coking, and restrains cracking reaction, while improving dehydrocyclisation reactions [11,14–17]. Also, it has been reported that the addition of alkaline earth metals as promoters neutralises surface acidity, inhibits coke deposition and increases the fraction of exposed metallic Pt surface after coke deposition [18–20]

* Corresponding author. Tel.: +33 467144620; fax: +33 46714 33 04.
E-mail address: melanie.taillades-jacquin@univ-montp2.fr (M. Taillades-Jacquin).

0926-3373/$ – see front matter © 2013 Elsevier B.V. All rights reserved.
http://dx.doi.org/10.1016/j.apcatb.2013.02.037

In previous studies, the activity of Pt and Pt-Sn based γ-Al_2O_3 on the dehydrogenation of Jet A-1 surrogate showed good H_2 productivity but exhibited limited thio-tolerance [21,22]. In these works, the addition of tin clearly improved the activity but a high loading of Sn [22] led to a decrease of both activity and stability. A significantly higher Pt loading did not improved the deactivation profile, but the catalyst co-impregnated with sodium as promoter, gave the highest and most sustained H_2 generation [21]. But these works were preliminary activity tests and it seems that no other works were reported on the catalytic dehydrogenation of kerosene. So in this present work we have investigated the influence of the nature of the support on the partial dehydrogenation of Ultra Low Sulfur Kerosene (ULSK) Jet A-1 using new Pt-Sn based catalysts. A series of catalysts, based on the 1%Pt 1%Sn/γ-Al_2O_3 material were developed with the modification of the γ-Al_2O_3 support by addition of hydrotalcite, CeO_2 and BaO promoters that are well known dopants in the automotive industry used to stabilze γ-Al_2O_3 from sintering, enable sulphur tolerance and increase activity [18–20]. The performances of these catalysts in the partial dehydrogenation reaction, the effects of different acidity, pore size and chemical composition were investigated.

The partial dehydrogenation produce H_2 that will directly feed the on-board fuel cell of a plane and a liquid phase, with original fuel properties to be reused as jet fuel.

2. Experimental

2.1. Catalyst preparation

Catalysts 1 wt.% Pt-1 wt.% Sn/γ-Al_2O_3, 1 wt.% Pt-1 wt.% Sn/20 wt.% CeO_2/γ-Al_2O_3, 1 wt.% Pt-1 wt.% Sn/MgAlO mixed oxide, 1 wt.% Pt-1 wt.% Sn/3 wt.% BaO-/γAl_2O_3, (hereinafter denoted PtSn/Al, PtSn/CeAl, PtSn/MgAlO and PtSn/BaAl respectively), were prepared by co-impregnation with Pt and Sn. This co-impregnation method was preferred to the successive impregnation method employed previously [21,22] in order to obtain a homogeneous distribution of the two metal particles. All alumina-based supports were supplied by Sasol. PtSn/Al utilised γ-Al_2O_3, PtSn/CeAl is γ-Al_2O_3 doped with 20% CeO_2, PtSn/MgAlO is a hydrotalcite-derived support that is a mixed magnesium aluminium oxide with 28% MgO, and PtSn/BaAl is γ-Al_2O_3 doped with 3% BaO. All supports were impregnated with a solution of the salts $Pt(NO_3)_4$ (Alfa Aesar) and $SnCl_2{\cdot}H_2O$ (Alfa Aesar). The resulting products were dried at 105 °C for 2 h and finally calcined in air at 550 °C (3 °C min^{-1}.) for 2 h.

2.2. Catalyst characterisation

X-ray powder diffraction (XRPD) patterns were recorded using a Philips PW 1050/81 goniometer, equipped with a PW 1710 unit, using Cu Kα radiation (λ = 0.15418 nm, 40 kW, 25 mA). N_2 adsorption/desorption isotherms were obtained using a Micromeritics ASAP 2020 M P volumetric adsorption system operating at 77 K. The samples were pre-treated by outgassing at 150 °C for 12 h under secondary vacuum. Specific surface area and mean pore diameter were calculated from the adsorption and desorption branches of the isotherms, respectively. The thermoprogrammed desorption of ammonia (NH3-TPD) method was used here to evaluate the surface acidity of the catalysts and the strength of acid sites. The parameter induced from this analyse is the quantity of ammonia irreversibly adsorbed at 150 °C and then removed from the sample surface between 150 and 900 °C. This quantity (μmol of NH_3 g^{-1}) represents the total acidity per mass unity of the sample. The measurements were performed in an Autochem 2910 by Micromeritics equipped with a TCD detector. The samples first underwent treatment for 1 h at 500 °C under He and were then submitted to a flow of 5% NH_3 in He (30 ml min^{-1}) at 150 °C until saturation, and then flushed with He at the same temperature for 1 h to eliminate NH_3 molecules physisorbed at the surface. Then, the thermoprogrammed desorption of NH_3 from the sample surface is done by heating the material from 150 to 900 °C with a heating rate of 10° min^{-1} under 30 ml min^{-1} He flow and analysed with the TCD detector. The accessible metal surface area was determined from H_2 chemisorption using a Micromeritics ASAP 2010C instrument. The sample was introduced into the measurement cell, which was flushed with helium. The sample was heated to 300 °C and reduced with hydrogen. The gas was then evacuated at the same temperature, and a second adsorption cycle carried out. Sample was first flushed in a flow of helium, and then evacuated before chemisorption with H_2 at 300 °C. The metal dispersion value so derived provides an estimation of the metal particle size through the relation: $D\% = 1000/d$, where $D\%$ is the metal dispersion and d is the metal particle diameter in Å.

2.3. Catalytic activity tests

Catalytic activity tests were performed in the gas phase in a pressurised fixed bed downward flow reactor on-line with a GC system (Agilent Technologies 7890A) equipped with TCD and FID detectors. The catalyst was loaded in the reactor in the form of compacted powders sieved to particles of 0.85–1.0 mm size. The catalysts were activated at 350 °C in a 40% H_2 in Ar flow at atmospheric pressure before use. The feed mixture composition was 93% Ultra Low Sulfur Jet A-1 Kerosene (denoted ULSK) (S < 3 ppm) in 7% H_2. This small stream of hydrogen was added into the feed to avoid coke deposition on the catalytic surface, as the hydrogen should clean the surface. The higher hydrogen partial pressure within the reaction zone will reduce the formation of coke precursor species, via hydrogen stabilization effect on the platinum metal centers (Z-type sites) and acidic centers on the support [23,24].

In this generation of hydrogen system, after the partial dehydrogenation step, the hydrogen will be purified by a pressure swing adsorption step and will be consumed as it is produced. For this, the operating pressure was set at 10 bar (rel.). The ULSK was fed by a HPLC pump, whereas the gas feed was guaranteed by Brooks Mass Flow Controllers; the outlet stream was monitored by a Brooks Mass Flow Meter. Tests were performed in the gas phase at 450 °C and using a contact time (τ) of 2 s. The exit stream of the reactor consisted of a two-phase mixture of a hydrogen-rich gas phase (with some light hydrocarbons) and liquid phase comprising unreacted ULSK and liquid reaction products. The stream then entered a phase separator where the liquid and gas phases were separated gravimetrically at room temperature. The liquid phase was collected at the end of each experiment in a fuel collection tank. This liquid composed of partially dehydrogenated hydrocarbons, maintains its original fuel properties and can be reused as jet fuel without a rehydrogenation step. The gas phase stream continuously exited the system, through a back-pressure regulator, to the GC system for gas phase analysis.

From each completed run, a portion of the used catalyst was collected for XRD measurements and carbon content analysis. Coke characterisation and quantification were performed using elemental and thermal analyses, and Raman spectroscopy. The carbon content was determined from total oxidation of the carbon by FLASH EA 1112 analyser. Thermal analyses were carried out with a NETZSCH STA409 PC thermobalance. The samples were heated to 800 °C (heating rate 2 °C min^{-1}) under air flow (20 ml min^{-1}). Raman spectra were obtained in backscattering geometry using a Horiba Jobin-Yvon LabRam Aramis IR^2 Raman spectrometer equipped with a red light gas laser (λ = 633 nm), an Olympus microscope, and a charge coupled device camera cooled by a

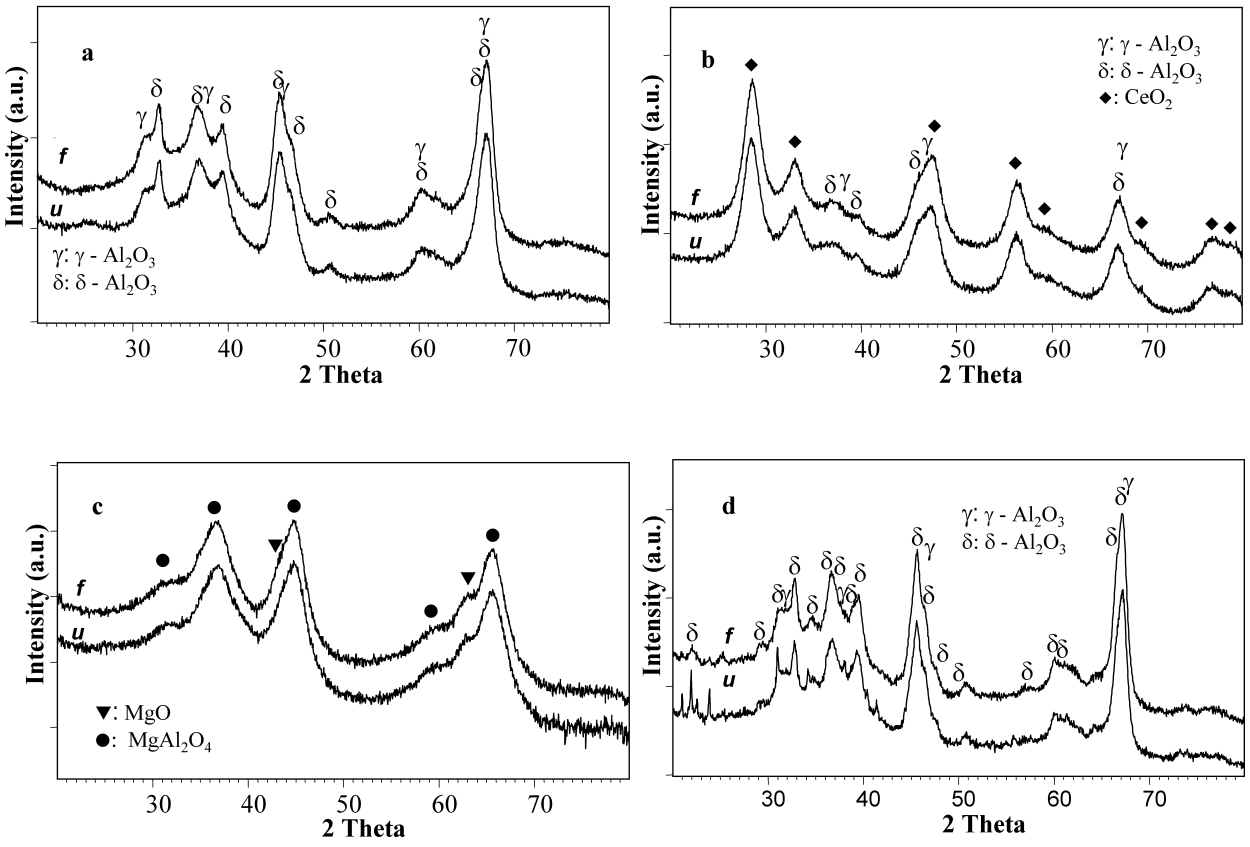

Fig. 1. XRD patterns of: (a) fresh (f) and used (u) PtSn/Al, (b) fresh (f) and used (u) PtSn/CeAl, (c) fresh (f) and used (u) PtSn/MgAlO, (d) fresh (f) and used (u) PtSn/BaAl.

thermoelectric Peltier device. The spectrometer was calibrated using Si. The laser power focused by the objective (×50) of microscope was near 10 mW on the sample surface

3. Results and discussion

3.1. Structural and surface characterisation

The diffraction patterns of fresh PtSn/Al, PtSn/CeAl, PtSn/MgAlO and PtSn/BaAl samples are shown in Fig. 1(a–d). Fig. 1a is the diffraction pattern of the fresh (f) PtSn/Al catalyst that is constituted of a mixture of δ and γ Al_2O_3 (ICDD File no 00-016-0394 and 00-029-0063 respectively); the broad XRD peaks indicate the low crystallinity of the support. Fig. 1b shows the diffraction pattern of the fresh (f) PtSn/CeAl catalyst. As for the PtSn/Al sample, no features from tin or platinum metal or oxides are visible. The diffraction peaks of CeO_2 (ICDD File no 00-034-0394), which is in concentration of 20 wt.%, are well evident, and the remaining lines can be attributed to δ and γ Al_2O_3 (ICDD File no 00-016-0394 and 00-029-0063 respectively). The broad XRD peaks of fresh PtSn/MgAlO (Fig. 1c (f)), can be attributed to $MgAl_2O_4$ (ICDD File no 00-021-1152) and to MgO (periclase) (ICDD File no 00-045-0946). The diffraction pattern (Fig. 1d (f)) of PtSn/BaAl is dominated by the phases δ and γ Al_2O_3 and no diffraction peaks of BaO, can be seen as it is in a too small concentration of 3 wt.% Again, no diffraction peaks of tin or platinum oxides or metals are seen.

The N_2 adsorption/desorption isotherm curves of PtSn/Al, PtSn/CeAl, PtSn/MgAlO and PtSn/BaAl are shown in Fig. 2a, b, c and d respectively, and the specific surface area and porosity values determined from these data are shown in Table 1. All catalysts have similar or lower surface area from 100 to 130 $m^2\,g^{-1}$ but higher pore diameter than catalysts in our previous works [21,22], except for PtSn/MgAlO with the highest surface of 230 $m^2\,g^{-1}$. The larger pore diameter can affect product selectivity and improve resistance to coke formation [25,26] as small pores can be filled with deposited carbon leading to problem diffusion and hence loss of activity. The N_2 adsorption/desorption isotherms of PtSn/Al (Fig. 2a) reveal a structure with pores in the range of mesoporosity (diameter 12 nm) with unimodal distribution. PtSn/CeAl has a bimodal pore distribution of diameter 5 and 8 nm. PtSn/MgAlO, has the least well-organised pore structure compared to the other three materials studied, as the N_2 adsorption/desorption isotherm curves (Fig. 2c) indicate, pore size covers a wide range whose mean value is 7 nm, although it has highest surface area of all four materials. The N_2 adsorption/desorption isotherm curves of PtSn/BaAl, shown in Fig. 2d, reveal a well organized pore structure with a unimodal pore size distribution. This catalyst has the highest pore diameter of 18 nm and the lowest specific surface area (100 $m^2\,g^{-1}$).

The surface acidity of our previous catalysts [21] was high and could favour cracking reactions due to acid sites on alumina [24]. Therefore, the strategy was to reduce the surface acidity of the support, to avoid excess coke. The values of acidity (μmoles of $NH_3\,g^{-1}$ of catalyst) of the samples PtSn/Al, PtSn/CeAl, PtSn/MgAlO and PtSn/BaAl are presented in Table 1 and the NH_3-TPD profiles of all samples are shown in Fig. 3. The total acidity of the non-modified alumina support PtSn/Al is 120 μmoles $NH_3\,g^{-1}$. The addition of an oxide phase to γ-Al_2O_3 seems to affect the total acidity: the presence of CeO_2 increases the acidity (PtSn/CeAl, 171 μmoles $NH_3\,g^{-1}$), while BaO decreases it (PtSn/BaAl, 101 μmoles $NH_3\,g^{-1}$). The sample PtSn/MgAlO, with a hydrotalcite derived support, has the highest acidity of 195 μmoles $NH_3\,g^{-1}$. Ammonia desorption from this sample gives rise to one peak at 260 °C of highest intensity, revealing the presence of medium strength acid sites. In the case of PtSn/CeAl and PtSn/Al, two peaks are observed at 260 and 400 °C,

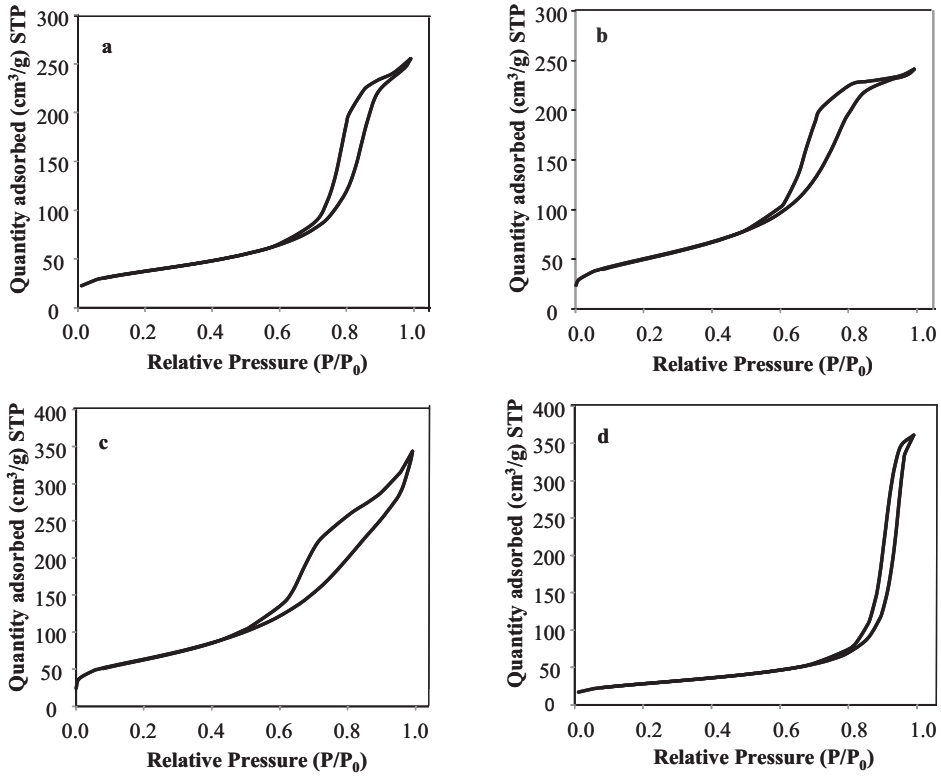

Fig. 2. N_2 adsorption/desorption isotherms of (a) PtSn/Al, (b) PtSn/CeAl, (c) PtSn/MgAlO and (d) PtSn/BaAl.

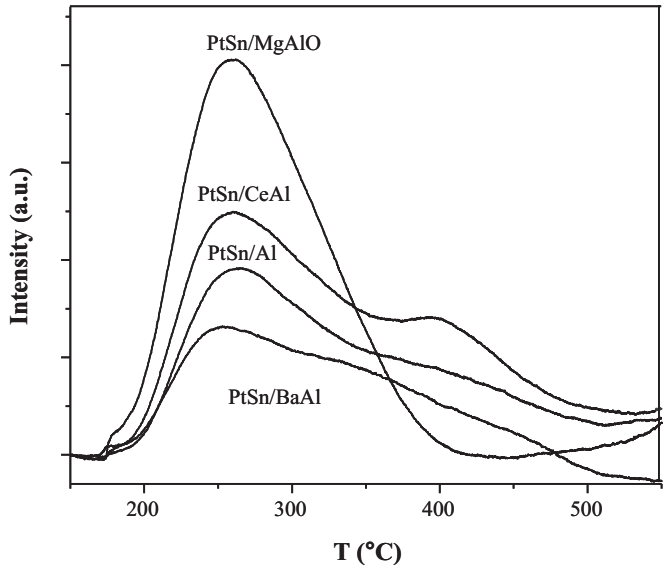

Fig. 3. Thermoprogrammed desorption of ammonia profiles of PtSn/Al, PtSn/CeAl, PtSn/MgAlO and PtSn/BaAl.

showing the presence of medium but also strong acid sites. In comparison to PtSn/Al, the addition of CeO_2 to the γ-Al_2O_3 support increases the intensity of the signal. PtSn/BaAl shows also two peaks but a shift towards lower temperature for the two peaks can be observed (250 and 350 °C), indicated that the addition of BaO results in a decrease of the desorption temperature and the intensity of the signal, i.e. the strength and the number of acid sites.

Depending on the support and on the preparation route of the catalysts, the metallic particle size and dispersion can be different and as the metals confer the dehydrogenation property of the materials, the activity of the catalysts can be affected. The metal dispersion and the metallic surface area of the three modified support catalysts have been measured by hydrogen chemisorption and compared to the non modified material (Table 1). The metallic particles in PtSn/Al are highly dispersed (53%) and very small, with an estimated value of 2 nm (through the relation: $D\% = 1000/d$, d in Å). This catalyst has also a very high metallic surface area meaning a high available catalytic surface. Looking at the values of the three modified support catalysts, even if the addition of a metal oxide leads to a decrease in dispersion and available metallic surface area and an increase in particle size, the materials prepared with the impregnation of CeO_2 or BaO still contain both small particles of 3 nm well dispersed. Their metallic surface area of 75 $m^2\ g^{-1}{}_{metal}$ should leads to a similar good activity in dehydrogenation. On the other side, PtSn/MgAlO prepared with a mixed oxide support,

Table 1
Characterisation data and catalyst performance.

Catalysts	S_{BET} ($m^2\ g^{-1}$)	Dp[a] (BJH, nm)	Acidity (μmole $NH_3\ g^{-1}$)	Dispersion (%)	S_{met} ($m^2\ g^{-1}$ met.)	H_2 purity[b] (vol.%)	C % (w/w)
PtSn/Al	130	12	120	53	128	94.5	8.4
PtSn/CeAl	180	5–8	171	31	75	96.0	2.3
PtSn/MgAlO	230	7	195	20	49	97.0	4.3
PtSn/BaAl	100	18	101	30	74	97.1	1.9

[a] Calculated from adsorption branch data.
[b] Average value obtained during reaction.

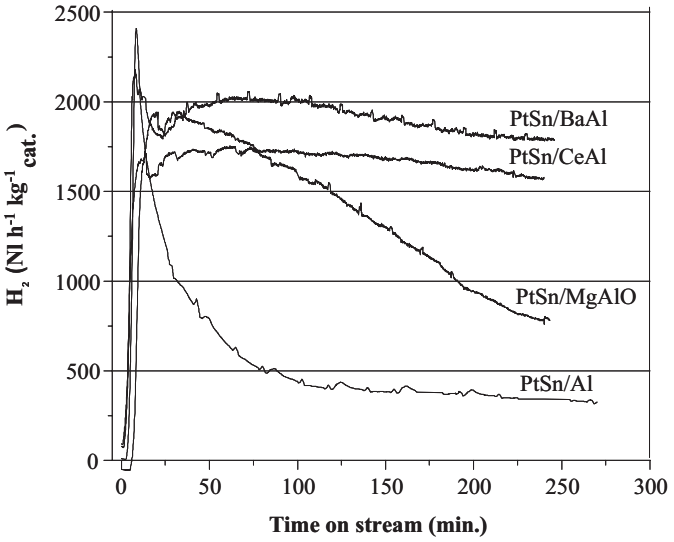

Fig. 4. Catalytic activity of PtSn/Al, PtSn/CeAl, PtSn/MgAlO and PtSn/BaAl in terms of H_2 productivity vs. time on stream, with ULSK Jet A-1 at 10 bar and 450° C.

shows a higher decrease in dispersion and a low metallic surface area, this catalyst is expected to have a low activity.

3.2. Catalytic activity tests

The results of the catalytic activity evaluation in terms of H_2 productivity vs. time on stream conducted at 10 bar at 450 °C with ULSK Jet A-1 on PtSn/Al, PtSn/CeAl, PtSn/MgAlO and PtSn/BaAl are shown in Fig. 4. The purity of the hydrogen obtained with each catalyst is reported in Table 1. High initial hydrogen production activity is given by all catalysts in the first 20 min and the hydrogen purity is in a 95–97% range, showing the potential of gas phase partial dehydrogenation. The gaz phases have been analysed in previous works [27] showing that the other components were light hydrocarbons (C1–C4) in low quantities. But as there is no oxygenated components in the composition of the kerosene and no water during the reaction, the gaz phase is free of CO or CO_2 impurities. PtSn/CeAl and PtSn/BaAl are observed to be more stable with time on stream than either PtSn/Al or PtSn/MgAlO, and to provide higher hydrogen production.

The PtSn/Al catalyst shows a peak of H_2 production of 2400 Nl kg_{cat}^{-1} h^{-1} in at the beginning of the reaction. However, the deactivation of this sample is fast and the productivity drops to 500 Nl kg_{cat}^{-1} h^{-1} in 1 h; at 250 min of time on stream hydrogen productivity is 350 Nl kg_{cat}^{-1} h^{-1}. This catalyst has the higher metal dipersion and higher metallic surface area, but also the second lowest acidity of all those examined. Therefore activity could be expected to be better and stable, and cracking reactions to be lower on the alumina acidic surface; and furthermore the relatively large pore diameter (12 nm) should have help to avoid coke deposition. So this fast deactivation due to coke formation is not linked to the surface properties of the material and has required further analysis in TGA. In the case of the PtSn/MgAlO catalyst, that has the mixed oxide support with the highest surface area and the highest acidity, the initial hydrogen productivity is 2000 Nl kg_{cat}^{-1} h^{-1}, however deactivation is responsible for a linear decrease to 800 Nl kg_{cat}^{-1} h^{-1} at the end of 250 min of time on stream. The deactivation can be related to the mixed oxide support and coke formation on the surface with a partial carbonation of MgO as well as to the presence of the spinel phase $MgAl_2O_4$ in the support. The two catalysts with an alumina support impregnated with Ce or Ba with an acidity of PtSn/CeAl higher than PtSn/BaAl,

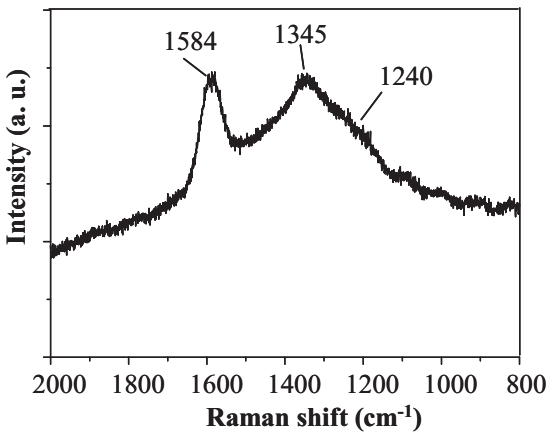

Fig. 5. Raman spectrum of a typical spent sample.

both yielded high hydrogen production with good stability (respectively 1700 Nl kg_{cat}^{-1} h^{-1} and 2000 Nl kg_{cat}^{-1} h^{-1} during the first 100 min, 1500 Nl kg_{cat}^{-1} h^{-1} and 1800 Nl kg_{cat}^{-1} h^{-1} at time on stream of 240 min). A linear extrapolation of hydrogen productivity to zero allows estimation of PtSn/CeAl lifetime of 23 h and PtSn/BaAl, 32 h both exceeding the extrapolated lifetime of the best catalyst on our previous works [21]. PtSn/BaAl has the lowest acidity, and the presence of BaO could provide better resistance to deactivation compared to the three other catalysts. PtSn/CeAl having a high acidity is also rather stable, which could be rationalised by the presence of cerium, which prevents strong adsorption of the hydrocarbon species that can lead to coke formation.

3.3. Coke characterisation and quantification

The deactivation process of the supported PtSn catalysts is complex and implicates multiple factors, of which coke deposition is for sure one. Analysis of the amount of deposited coke and the H_2 productivity curves reveals that the catalyst lifetime is directly related to coke formation, since the higher the amount of coke deposited, the faster is the deactivation in H_2 production.

The coke formed during the dehydrogenation reaction has been characterised and quantified. All the used samples were submitted to thermal treatment at 300 °C under vacuum for 4 h to desorb all traces of unreacted kerosene condensed on the powder during the reactor shut-down, this procedure was necessary for reliable characterisation and quantification.

The diffraction patterns of used PtSn/Al, PtSn/CeAl, PtSn/MgAlO and PtSn/BaAl samples are given in Fig. 1(a–d) and can be compared to those obtained with the fresh samples. The diffraction pattern of the used PtSn/Al, PtSn/CeAl and PtSn/MgAlO (Fig. 1a–c (u)) are the same as those of the fresh catalysts. No diffraction peaks of tin or platinum oxides, or metallic tin or platinum may be seen probably due to their low concentration. In Fig. 1d (u), the diffraction pattern of used PtSn/BaAl shows sharper peaks revealing an increase of the domain size during catalyst usage, with a few XRD features being more resolved than in the pattern of the fresh sample but given the complexity of the diffraction pattern they have not been assigned.

Raman spectroscopy provides qualitative informations on the nature of the deposited carbon. Fig. 5 is the Raman spectrum of typical used sample, all the other samples showed similar spectra, meaning that for the four catalysts the nature of the deposited carbon is the same. Three main features, at 1584 cm^{-1}, 1345 cm^{-1} (broad line) and a shoulder at 1240 cm^{-1} can be observed. The line at 1584 cm^{-1} is a stretching vibration (G mode) which can be attributed to any pair of sp^2 sites whether in C=C chains or in aromatic rings. The band at 1345 cm^{-1} is a breathing vibration

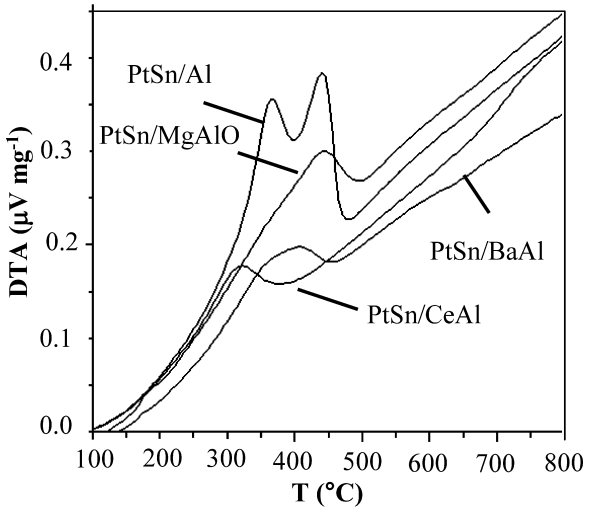

Fig. 6. Differential thermal analysis curves obtained with PtSn/Al, PtSn/CeAl, PtSn/MgAlO and PtSn/BaAl catalysts.

of sp^2 sites (D mode) only in rings not in chains. The shoulder at 1240 cm^{-1} can be ascribed to C—H vibrations. The deposited carbon on all catalyst surfaces is mainly graphitic.

The extent of carbon deposition on each sample has been determined by carbon total oxidation, and the results are shown in Table 1. The amount of carbon on the catalyst surface is directly correlated with the deactivation rate of each catalyst. PtSn/Al has the highest carbon content and the lowest H_2 productivity and stability. This is the only catalyst not modified by the presence of a second oxide, that would suggest, first of all that even reduced surface acidity and large pore size did not avoid coke formation on the catalyst and then, that an additional metal oxide helps prevent coke deposition. PtSn/MgAlO deactivated quickly and also has a high amount of coke deposition, meaning that this oxide support highly acidic leading to low metal dispersion do not avoid coke deposition. PtSn/CeAl and PtSn/BaAl have lower amounts of deposited carbon, and of these PtSn/BaAl shows the highest H_2 productivity and the greatest stability as well as the lowest deposited coke content. These results are in accordance with those found by Yu et al., Vu et al. and [28,29], the stability of the catalyst during the reaction exhibited different tolerances according to the support used and the presence of Ce or Ba stabilized the active states of Pt, Sn and support but also supress the coke accumulation on the catalyst during the reaction and improve the catalytic performances.

The TGA analysis curves shown in Fig. 6 allowed understanding the coke mechanism deposition on each catalyst. The DTA curve reveals one or two exothermic peaks, the whole oxidation process occurs between 200 °C and 570 °C. Liu et al. [30] have concluded that the deposited carbon species burnt at low temperature are mainly those formed on metal sites, while the coke burnt at high temperature is primarily deposited on the Brønsted acid sites and is responsible for the gradual deactivation of the catalyst. The catalyst PtSn/Al showed two peaks of high intensity and according to this interpretation, coke is deposited on the metal sites and also support area with a peak of higher intensity at high temperature. This explains the rapid deactivation of this material but also its low activity in the partial dehydrogenation of kerosene. PtSn/MgAlO showed only a shoulder at low temperature and a peak at higher temperature meaning that the modification of the support with MgO tends to increase coke deposition on the acidic sites of the support and is responsible for the rapid deactivation. PtSn/CeAl has only one peak at lower temperature, of lower intensity. This suggests that CeO_2 addition prevents surface coke deposition on the support acid sites, which has the results of slowing down the deactivation. In the case of PtSn/BaAl, a single peak of low intensity is observed, the maximum of which is shifted to a temperature intermediate between those observed for the PtSn/Al support for example. This corresponds to an increase in the temperature at which coke deposited on metal sites is removed, and a decrease in the temperature at which coke deposited on acidic sites is oxidised. As observed above, the presence of BaO limits coke deposition, probably more on the metal sites, as suggested by the lowest deactivation rate of this catalyst.

4. Conclusions

The objective of this research was to investigate the influence of the nature of the support of Pt-Sn/Al_2O_3 based catalysts on hydrogen generation by partial dehydrogenation of kerosene. The alumina support has been modified by magnesium, cerium and barium oxides, which have different effects on the support acidity and which can provide other advantageous properties such as inhibition of metal particle sintering. The performance of these catalysts, the effects of different acidity and textural properties have been investigated and compared with the non modified support 1 wt.% Pt-1 wt.% Sn/γ-Al_2O_3.

The results show that the dopants do not change the structure of the support but modify the acidity and this modification is strongly dependant on the nature of the dopant. A comparison of the trends in H_2 productivity and amount of coke deposited at a given time on stream reveals that the higher is the degree of coke deposited the faster is the deactivation in H_2 production. Addition of a specific dopant can prevent surface coke deposition on the support and slow down the deactivation.

A catalyst with Al_2O_3 doped with 3% BaO presents the lowest surface acidity and promising results in the partial dehydrogenation of ULSK JET A-1 with productivity of 2000 $NL_{H2}\ kg_{cat}^{-1}\ h^{-1}$ of H_2 purity 97 vol.%. This catalyst is more stable, and gives higher hydrogen production activity, than the catalyst without dopant. Further improvement of this material, in particular by investigation the effect of the Pt/Sn ratio on the nature of the alloy formed and on catalyst activity will be the objective of our future studies.

Acknowledgment

Financial support by the EU–FP7 for the GreenAir project–Grant Agreement No. 233862 – is acknowledged with thanks.

References

[1] S.G. Chalk, J.F. Miller, Journal of Power Sources 159 (2006) 73–80.
[2] S. Satyapal, J. Petrovic, C. Read, G. Thomas, G. Ordaz, Catalysis Today 120 (2007) 246–256.
[3] H.L. Hellman, R. van den Hoed, International Journal of Hydrogen Energy 32 (2007) 305–315.
[4] R.B. Biniwale, S. Rayalu, S. Devotta, M. Ichikawa, International Journal of Hydrogen Energy 33 (2008) 360–365.
[5] C.L. Aardahl, S.D. Rassat, International Journal of Hydrogen Energy 34 (2009) 6676–6683.
[6] M.P. Lazaro, E. Garcia-Bordejé, D. Sebastian, M.J. Lazaro, R. Moliner, Catalysis Today 138 (2008) 203–209.
[7] Y. Okada, E. Sasaki, E. Watanabe, S. Hyodo, H. Nishijima, International Journal of Hydrogen Energy 31 (2006) 1348–1356.
[8] Y. Saito, K. Aramaki, S. Hodoshima, M. Saito, A. Shono, J. Kuwano, Chemical Engineering Science 63 (2008) 4935–4941.
[9] S. Hodoshima, S. Takaiwa, A. Shono, K. Satoh, Y. Saito, Applied Catalysis A-General 283 (2005) 235–242.
[10] P. Jänker, F. Nitschké, C. Wolff, US Patent No. 20090274615A1, assigned to Airbus Deutschland GmbH (2009).
[11] B. Wang, G.F. Froment, D. Wayne Goodman, Journal of Catalysis 253 (2008) 239–243.
[12] N. Kariya, A. Fukuoka, M. Ichikawa, Applied Catalysis A-General 233 (2002) 91–102.

[13] D. Sebastian, E.G. Bordejé, L. Calvillo, M.J. Lazaro, R. Moliner, International Journal of Hydrogen Energy 33 (2008) 1329–1334.
[14] Y.K. Park, F.H. Ribeiro, G.A. Somorjai, Journal of Catalysis 178 (1998) 66–75.
[15] M.P. González-Marcos, B. Iñarra, J.M. Guil, M.A. Gutiérrez-Ortiz, Catalysis Today 107–108 (2005) 685–692.
[16] M.P. González-Marcos, B. Iñarra, J.M. Guil, M.A. Gutiérrez-Ortiz, Applied Catalysis A 273 (2004) 259–268.
[17] F.B. Passos, D.A.G. Aranda, M. Schmal, Journal of Catalysis 178 (1998) 478–488.
[18] P.K. Cheekatamarla, C.M. Finnerty, Journal of Power Sources 160 (2006) 490–499.
[19] R.J. Farrauto, R.M. Heck, Catalysis Today 51 (3–4) (1999) 351–360.
[20] J. Kašpar, P. Fornasiero, N. Hickey, Catalysis Today 77 (2003) 419–449.
[21] C. Resini, C. Lucarelli, M. Taillades-Jacquin, K. Liew, I. Gabellini, S. Albonetti, D. Wails, J. Rozière, A. Vaccari, D. Jones, International Journal of Hydrogen Energy 36 (10) (2011) 5972–5982.
[22] C. Lucarelli, S. Albonetti, A. Vaccari, C. Resini, G. Taillades, J. Roziere, K. Liew, A. Ohnesorge, C. Wolff, I. Gabellini, D. Wails, Catalysis Today 175 (1) (2011) 504–508.
[23] D. Sanfilippo, I. Miracca, Catalysis Today 111 (2006) 133–139.
[24] K. Kumbilieva, N.A. Gaidai, N.V. Nekrasov, L. Petrov, A.L. Lapidus, Chemical Engineering Journal 120 (2006) 25–32.
[25] G. Ertl, H. Knoezinger, J. Weitkamp, Handbook of Heterogeneous Catalysis, vol. 1–5, Wiley-VCH, Germany, 1997, ISBN 3-527-29212-8.
[26] S. Ghosh, S. Makhija, M. Santra, V. Krishnan, K. Mohan Prabhu, V.L.N. Murthy, M. Rama Rao, S.K. Ray, Studies in Surface Science and Catalysis 113 (1998) 271–276.
[27] K. Liew, Ph.D. thesis « Fundamentals of Partial Dehydrogenation: Theoretical and Experimental Investigation on a New Fuel Processing Method to Generate Hydrogen from Jet Fuel » 2011.
[28] C. Yu, Q. Ge, H. Xu, W. Li, Applied Catalysis A-General 315 (2006) 58–67.
[29] B.K. Vu, M.B. Song, I. Ahn, Y. Suh, D.J. Suh, W. Kim, H. Koh, Y.G. Choi, E.W. Shin, Catalysis Today 164 (2011) 214–220.
[30] B.S. Liu, L. Jiang, H. Sun, C.T. Au, Applied Surface Science 253 (11) (2007) 5092–5100.